

# Role of Turbulence in Wake-Induced Galloping of Transmission Lines

Andrew N. Hoover\* and Roger J. Hawks†  
Clarkson College of Technology, Potsdam, N. Y.

Linearized equations of motion are used in conjunction with power spectral analysis to analyze full-span oscillations of smooth two-conductor bundle transmission lines in turbulent winds. Assuming a von Karman model for low-altitude turbulence, it is found that, for low wind speeds, the response of the bundle is small for all equilibrium bundle tilt angles. As wind speed increases large-amplitude motions occur for tilt angles near  $10^\circ$ . These motions begin as horizontal galloping, but vertical galloping dominates for high wind speeds. Bundle rolling occurs only at the highest wind speeds considered.

## Nomenclature

$C_{L0}, C_{D0}, C_{m0}$	= aerodynamic coefficients at equilibrium
$C_{L\gamma}, C_{D\gamma}, C_{m\gamma}$	= slopes of aerodynamic coefficients with respect to angle of attack
$C_{m\dot{q}}$	= aerodynamic roll damping coefficient
$c$	= conductor diameter
$D$	= $d/d\hat{t}$
$D_f$	= aerodynamic drag force
$d$	= conductor separation
$F_x, F_z$	= aerodynamic forces per unit length
$G$	= transfer function
$g$	= acceleration of gravity
$h$	= height of bundle above ground
$i$	= $(-1)^{1/2}$
$L$	= scale length of turbulence
$L_f$	= aerodynamic lift force
$M_y$	= aerodynamic moment per unit length
$m$	= bundle mass per unit length
$q$	= dynamic pressure; $q = 1/2 \rho V^2$
$t$	= time
$t^*$	= reference time; $t^* = d/V$
$u_r, w_r$	= random components of wind velocity
$V$	= mean wind velocity
$V_c$	= wind velocity relative to bundle
$x_0, z_0, \theta_0$	= time variation of bundle displacement
$\alpha$	= bundle-equilibrium tilt angle
$\gamma$	= relative wind angle
$\theta$	= angle between bundle and horizontal
$\Lambda$	= total angle of attack
$\mu$	= relative mass; $\mu = \rho c d / 2m$
$\rho$	= air density
$\sigma$	= rms value of random wind component
$\Phi$	= power spectral density
$\Omega$	= turbulent wave number
$\omega_x, \omega_z, \omega_\theta$	= structural natural frequencies of bundle

## Superscripts

.	= $d/dt$
^	= dimensionless quantity
*	= complex conjugate

## Introduction

TRANSMISSION-line galloping is a full-span, wind-induced oscillation that occurs with reduced frequencies that are small compared to the wake Strouhal number. Thus, this oscillation arises from quasisteady rather than unsteady aerodynamic forces. Galloping usually involves large amplitudes and low frequencies. Single-conductor galloping develops from changes in the conductor lift<sup>1</sup> or drag<sup>2</sup> due to variations in the conductor cross section. In multiple- or bundle-conductor lines galloping is caused by wake interference effects between the smooth circular conductors. This wake-induced galloping has been studied by Simpson and Lawson<sup>3</sup> and Brzozowski and Hawks.<sup>4</sup>

The previous studies of wake-induced galloping have concentrated on the stability of the bundle in a uniform wind. It was assumed that the oscillation was self-starting and that any turbulence in the wind would tend to break up the wake, thus damping the oscillation. However it has been shown<sup>5</sup> that turbulence can greatly effect the galloping motions of single non-circular sections. In this paper, we show that long-wavelength wind turbulence provides a mechanism for starting galloping in bundle conductors. Furthermore, we show that continued galloping is only possible for certain combinations of wind speed and bundle tilt angle.

## Analysis

If the transmission line is assumed to be a taut bundle with rigid, massless spacers and fixed ends (Fig. 1), the basic equations of motion are<sup>4</sup>

$$\ddot{x}_0 + \omega_x^2 x_0 = F_x / m \quad (1a)$$

$$\ddot{z}_0 + \omega_z^2 z_0 = F_z / m + 1/2 \pi g \quad (1b)$$

$$\ddot{\theta}_0 + \omega_\theta^2 \theta_0 = 4M_y / m d^2 \quad (1c)$$

These lumped parameter equations assume that only one of the structural natural frequencies of the cable is excited.

The aerodynamic forces arise from wake interactions between the conductors in the bundle. In the present case, the bundle consists of two smooth circular conductors (Fig. 2). When the leeward conductor is in the wake of the windward conductor, the aerodynamic forces act to move the leeward conductor toward the windward conductor and also toward the center of the wake. Since the conductors are separated by rigid spacers, these aerodynamic forces result in a lift force and a rolling moment on the bundle. Due to their dependence on the wake structure, these forces are functions of the wind speed and the relative wind angle. There is also some evi-

Received May 26, 1976; revision received Oct. 6, 1976.

Index category: Aeroelasticity and Hydroelasticity.

\*Research assistant, Dept. of Mechanical and Industrial Engineering. Presently with E. I. DuPont de Nemours & Co., Wilmington, Delaware. Student Member AIAA.

†Assistant Professor, Dept. of Mechanical and Industrial Engineering. Member AIAA.

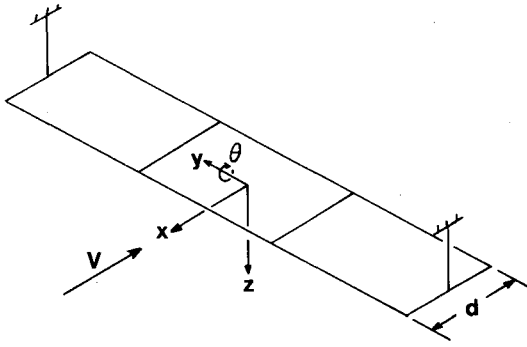


Fig. 1 Bundle geometry.

dence<sup>6</sup> that the aerodynamic forces are functions of the turbulence level.

The wind is modeled as a mean horizontal wind of velocity  $V$  with small superimposed random components  $u_r$  and  $w_r$ . The spanwise component of wind has a very small effect on the aerodynamics in comparison with the cross flow and is ignored. The relative wind angle for the bundle thus is

$$\gamma = \tan^{-1} [(w_r + \dot{z}_0) / (V + u_r + \dot{x}_0)] \quad (2)$$

$$[C] = \begin{bmatrix} D^2 + 2\mu C_{D0} D + \dot{\omega}_x^2 & \mu(C_{D\gamma} - C_{L0}) D & \mu C_{D\gamma} \\ 2\mu C_{L0} D & D^2 + \mu(C_{D0} + C_{L\gamma}) D + \dot{\omega}_z^2 & \mu C_{L\gamma} \\ -8\mu C_{m0} D & -4\mu C_{m\gamma} D & D^2 - 4\mu C_{mq} D + \dot{\omega}_\theta^2 - 4\mu C_{m\gamma} \end{bmatrix} \quad (10a)$$

which reduces to

$$\gamma = (w_r + \dot{z}_0) / V \quad (3)$$

since the turbulence is small. The total angle of attack of the bundle also depends on the roll angle. Thus

$$\Lambda = \gamma + \theta_0 \quad (4)$$

Aerodynamic coefficients for the bundle are defined as

$$L_f = \frac{1}{2} \rho V_c^2 c C_L \quad (5a)$$

$$D_f = \frac{1}{2} \rho V_c^2 c C_D \quad (5b)$$

$$M_y = \frac{1}{2} \rho V_c^2 c d C_m \quad (5c)$$

where

$$V_c^2 = (V + u_r + \dot{x}_0)^2 + (w_r + \dot{z}_0)^2 \quad (6)$$

If the motion is restricted to small disturbances from the equilibrium position, the aerodynamic coefficients can be linearized so that

$$C_L = C_{L0} + C_{L\gamma} \Lambda \quad (7a)$$

$$C_D = C_{D0} + C_{D\gamma} \Lambda \quad (7b)$$

$$C_m = C_{m0} + C_{m\gamma} \Lambda + C_{mq} \dot{\theta}_0 t^* \quad (7c)$$

For the small turbulence levels assumed, these coefficients depend only on wind speed and the angle of attack at equilibrium.

The roll-damping coefficient  $C_{mq}$  is produced by the drag on the individual conductors in the bundle and thus depends only on wind speed. This term was ignored in the previous studies. The total angle of attack at equilibrium is called the

bundle tilt angle. The tilt angle is determined primarily by the angle at which the bundle is hung from the support towers, but blow-back effects are also included.

Using Eqs. (3-7), the aerodynamic loads on the bundle can be written

$$F_x = qc [-C_{D0} - 2C_{D0} \dot{x}_0 / V + (C_{L0} - C_{D\gamma}) \dot{z}_0 / V - C_{D\gamma} \theta_0 - 2C_{D0} u_r / V + (C_{L0} - C_{D\gamma}) w_r / V] \quad (8a)$$

$$F_z = -qc [C_{L0} + 2C_{L0} \dot{x}_0 / V + (C_{L\gamma} + C_{D0}) \dot{z}_0 / V + C_{L\gamma} \theta_0 + 2C_{L0} u_r / V + (C_{L\gamma} + C_{D0}) w_r / V] \quad (8b)$$

$$M_y = qdc [C_{m0} + 2C_{m0} \dot{x}_0 / V + C_{m\gamma} \dot{z}_0 / V + C_{mq} \dot{\theta}_0 + C_{m\gamma} \theta_0 + 2C_{m0} u_r / V + C_{m\gamma} w_r / V] \quad (8c)$$

Nondimensionalizing by using the conductor spacing  $d$  and mean wind speed  $V$  as reference quantities, the equations of motion for the bundle become

$$[C] \begin{Bmatrix} \hat{x} \\ \hat{z} \\ \hat{\theta} \end{Bmatrix} = K_1 + K_2 \hat{u} + K_3 \hat{w} \quad (9)$$

where

$$K_1 = \mu \begin{bmatrix} -C_{D0} \\ \hat{g} - C_{L0} \\ 4C_{m0} \end{bmatrix} \quad (10b)$$

$$K_2 = 2\mu \begin{bmatrix} -C_{D0} \\ -C_{L0} \\ 4C_{m0} \end{bmatrix} \quad (10c)$$

$$K_3 = \mu \begin{bmatrix} C_{L0} - C_{D\gamma} \\ -(C_{D0} + C_{L\gamma}) \\ 4C_{m\gamma} \end{bmatrix} \quad (10d)$$

The random components of the wind are given in terms of power spectral densities. For example,

$$\sigma_u^2 = 2 \int_0^\infty \Phi_{uu}(\Omega) d\Omega \quad (11)$$

Since a lumped parameter model of the line is used in Eq. (9), spanwise variations of the wind will not influence the motion.

Based on the extensive data for low-altitude turbulence, Etkin<sup>7</sup> has adopted the von Karman spectra for wind-induced turbulence near the ground. Hence

$$\Phi_{uu} = \sigma_u^2 L / \pi [1 + (1.339 L \Omega)^2]^{5/6} \quad (12a)$$

$$\Phi_{ww} = \sigma_w^2 L [1 + 8/3 (1.339 L \Omega)^2] / 2\pi [1 + (1.339 L \Omega)^2]^{11/6} \quad (12b)$$

$$\Phi_{uw} = \frac{1}{2} \sigma_u \sigma_w [\Phi_{uu} \Phi_{ww} / \sigma_u^2 \sigma_w^2 (1 + L' \Omega^2 / 10)]^{1/2} \quad (12c)$$

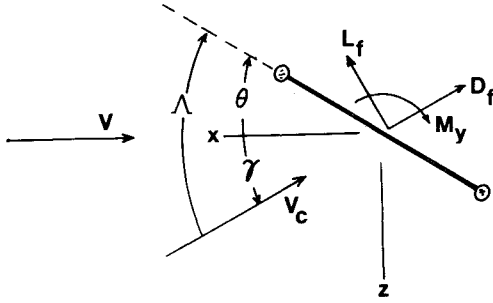


Fig. 2 Aerodynamic load on the bundle.

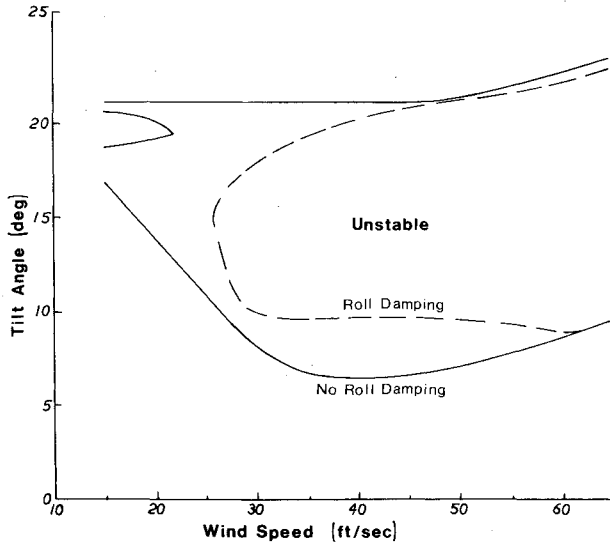


Fig. 3 Effect of roll damping on stability.

where, close to the ground, the intensity of the vertical component of turbulence  $\sigma_w$  is half the horizontal component  $\sigma_u$  and the scale lengths of the turbulence are related to the height by

$$L = 20h^{1/2} \quad L' = 0.4h \quad (13)$$

The power spectral response of the transmission line is calculated from the power spectrum of the wind by use of the transfer functions for the system, which are obtained from the equations of motion (9). Therefore

$$\begin{aligned} \Phi_{xx}(\Omega) = & |G_{xu}(\hat{\Omega})|^2 \Phi_{uu}(\Omega) + |G_{xw}(\hat{\Omega})|^2 \Phi_{ww}(\Omega) \\ & + |G_{xu}^*(\hat{\Omega}) G_{xw}(\hat{\Omega}) + G_{xw}^*(\hat{\Omega}) G_{xu}(\hat{\Omega})| \Phi_{uw}(\Omega) \end{aligned} \quad (14)$$

Similar expressions give  $\Phi_{zz}$  and  $\Phi_{\theta\theta}$ .

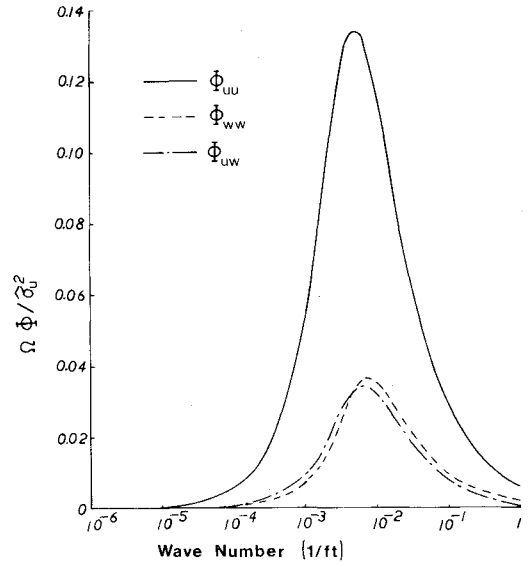
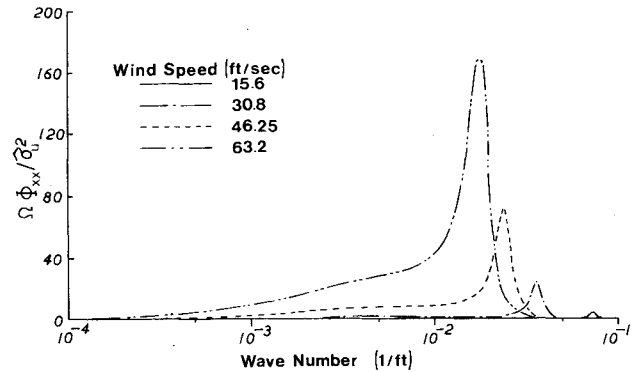
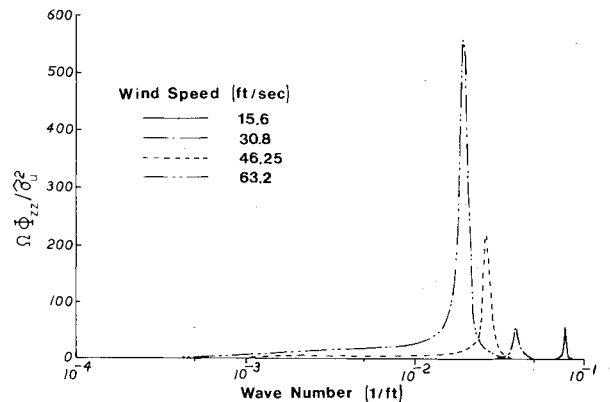
### Results

Calculations were made for a bundle of two smooth conductors with a 10-diameter separation ( $d/c=10$ ). The aerodynamic coefficients for this bundle were determined by Brzozowski and Hawks<sup>4</sup> from the wind-tunnel data of Wardlaw and Cooper.<sup>8</sup> This bundle has natural frequencies of

$$\omega_x = 1.10 \quad \omega_z = 1.221 \quad \omega_\theta = 1.528$$

in radians per second and is hung at a mean height  $h$  of 76 ft.

The previous studies of wake-induced galloping have ignored the roll-damping term  $C_{m\dot{\theta}}$ . Without roll damping, the bundle is only neutrally stable for large tilt angles, where the leeward conductor is outside the wake. Since field tests<sup>9</sup> show that galloping does not occur at large tilt angles, the ef-

Fig. 4 Wind power spectrum;  $h = 76$  ft.Fig. 5 Horizontal displacement power spectrum;  $\alpha = 15^\circ$ .Fig. 6 Vertical displacement power spectrum;  $\alpha = 15^\circ$ .

fect of roll damping on bundle stability was investigated. Figure 3 shows the result of this calculation. With roll damping included, the size of the unstable region is greatly reduced, and a critical speed appears. Thus galloping will not occur for wind speeds below about 25 fps at any tilt angle.

The power spectral densities for the turbulent wind acting on the transmission line are shown in Fig. 4. At the height of the line, the majority of the turbulent energy of the wind is in the wavelengths between 60 and 6000 ft. Unsteady aerodynamic effects are produced by turbulent wavelengths of the same order of magnitude as the conductor separation. Hence, these short wavelengths must be excluded. This produces only a small error in the results, however, since there is little wind energy at these wavelengths.

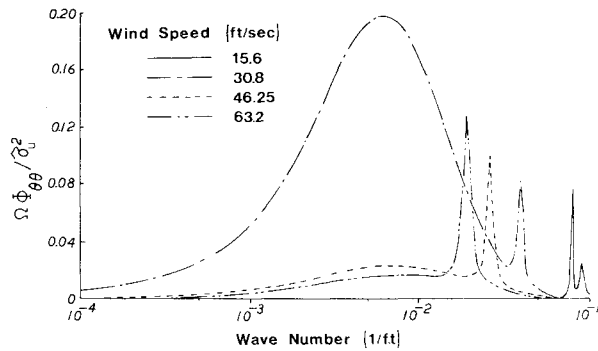
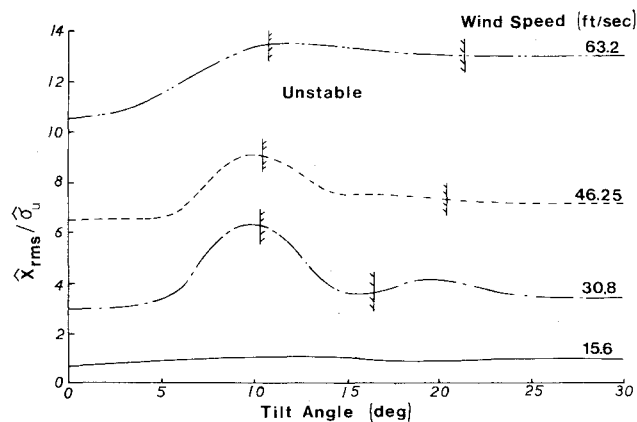
Fig. 7 Torsional displacement power spectrum;  $\alpha = 15^\circ$ .

Fig. 8 RMS horizontal displacement.

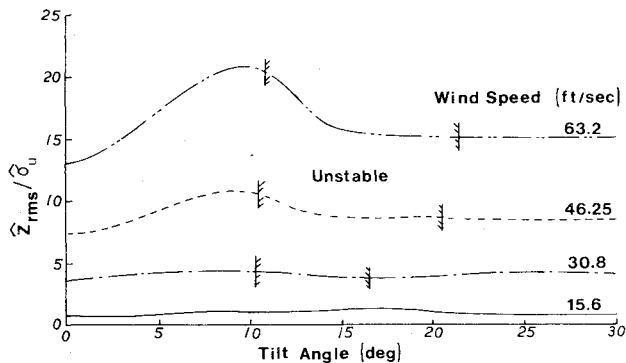


Fig. 9 RMS vertical displacement.

The power spectra for the displacements of the bundle are shown in Figs. 5-7 for a representative tilt angle of  $15^\circ$ . Most of the translational energy of the bundle is at the natural frequencies of the system. At low wind speeds, the aeroelastic natural frequency is at short wavelengths where the turbulent energy is small. As wind speed increases, the aeroelastic natural frequency shifts to longer wavelengths with a corresponding increase in output energy. There is also a slight contribution to bundle response from the input wind energy at longer wavelengths. The torsional mode behaves in a similar manner at this bundle tilt angle. The aeroelastic natural frequency shifts to longer wavelengths as wind speed increases. The bundle response at all but the lowest wind speed derives much of its energy directly from the turbulent wind energy (Fig. 7).

RMS values for the bundle displacement were obtained by integrating the power spectral densities. The rms displacements are shown in Figs. 8-10. These curves show that the dimensionless displacement in all three degrees of freedom is fairly constant for all bundle tilt angles at the lowest wind

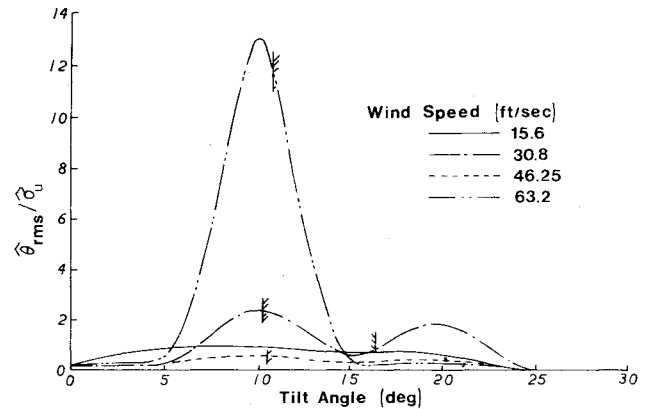
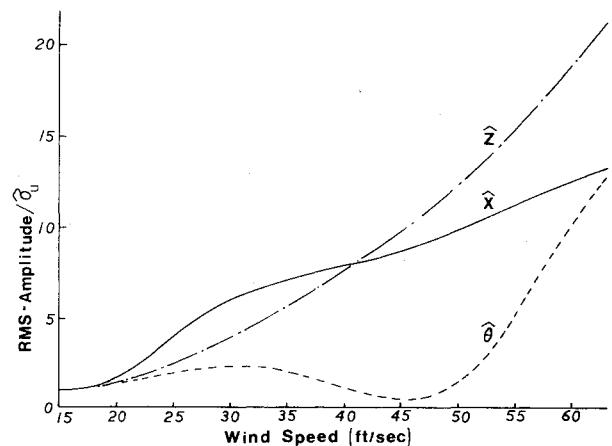


Fig. 10 RMS torsional displacement.

Fig. 11 Amplitude of galloping at  $\alpha = 10^\circ$ .

speed considered. Since this speed is below the critical speed, galloping does not occur, and the bundle follows the wind.

At a wind speed of 30.8 fps, peaks develop in the horizontal and rolling modes at a bundle tilt of  $10^\circ$ . This tilt angle is just outside the unstable region. Thus galloping occurs for a nominally stable line. The turbulence-induced motions will grow for unstable tilt angles. Hence wind turbulence provides the trigger for unstable galloping. At 30.8 fps, the translational modes dominate the bundle motion with an appreciable response in roll. The bundle motion at 46.25 fps is characterized by a negligible response in roll and maximum displacement in the vertical mode at  $10^\circ$ . For the highest wind speed considered, the vertical mode predominates with very large torsional displacements. Large-amplitude vibrations are possible in all modes at high wind speeds in the tilt angle range  $7-13^\circ$ . Field observations tend to confirm this result.

Since all three modes develop galloping for the stable tilt angle of  $10^\circ$ , Fig. 11 is a plot of the amplitude of each degree of freedom as a function of mean wind speed at this tilt angle. At low speeds, the response is primarily horizontal, whereas, at high speeds, the vertical mode tends to dominate with large torsional response.

### Conclusions

Calculations made with a linearized model of a bundle conductor transmission line have shown that wake-induced galloping does not occur for wind speeds below a critical speed. Above the critical speed finite amplitude galloping will occur due to wind turbulence for tilt angles less than those required for galloping instability. The galloping amplitude in this case increases with wind speed.

In the unstable region, wind turbulence starts a galloping motion which, in this linearized analysis, grows without bound. In an actual line, the nonlinearities in the aerodynamic

forces will act to limit the galloping amplitudes. Structural damping will also produce small changes in the instability boundaries and will reduce the amplitude of the stable galloping.

For low wind speeds the galloping motion is primarily horizontal. As wind speed increases, vertical galloping dominates, but torsional galloping only occurs for the highest wind speeds considered.

### Acknowledgment

This work was supported by a grant from the Alcoa Foundation.

### References

<sup>1</sup>Den Hartog, J. P., *Mechanical Vibrations*, McGraw-Hill, New York, 1956, pp. 299-305.

<sup>2</sup>Simpson, A., "Aerodynamic Instability of Long-Span Transmission Lines," *Proceedings of the Institute of Electrical Engineers*, Vol. 112, Feb. 1965, pp. 315-324.

<sup>3</sup>Simpson, A. and Lawson, T. V., "Oscillations of 'Twin' Power Transmission Lines," *Proceedings of the Symposium on Wind Effects on Buildings and Structures*, Loughborough University, April 1968.

<sup>4</sup>Brzozowski, V. J. and Hawks, R. J., "Wake Induced Full-Span Instability of Bundle Conductor Transmission Lines," *AIAA Journal*, Vol. 14, Feb. 1976, pp. 179-184.

<sup>5</sup>Novak, M. and Tanaka, H., "Effect of Turbulence on Galloping Instability," *Journal of the Engineering Mechanics Div. ASCE*, Vol. 100, No. EM1, Feb. 1974, pp. 27-47.

<sup>6</sup>Price, S. J., "Wake Induced Flutter of Power Transmission Conductors," *Journal of Sound and Vibration*, Vol. 38, Jan. 1975, pp. 125-147.

<sup>7</sup>Etkin, B., *Dynamics of Atmospheric Flight*, Wiley, New York, 1972, pp. 531-543.

<sup>8</sup>Wardlaw, R. L. and Cooper, K. R., "A Wind Tunnel Investigation of the Steady Aerodynamic Forces on Smooth and Stranded Twin Bundled Power Conductors for the Aluminum Company of America," LTR-LA-117, Aug. 1973, National Aeronautical Establishment, Ottawa, Canada.

<sup>9</sup>Mohajery, M., "Tests of Wake-Induced Oscillations of Bundle Conductors in Natural Winds," Tech. Rept. 20, 1975, Alcoa Laboratories, Pittsburgh, Pa.

## *From the AIAA Progress in Astronautics and Aeronautics Series . . .*

### **THERMAL POLLUTION ANALYSIS—v. 36**

*Edited by Joseph A. Schetz, Virginia Polytechnic Institute and State University*

This volume presents seventeen papers concerned with the state-of-the-art in dealing with the unnatural heating of waterways by industrial discharges, principally condenser cooling water attendant to electric power generation. The term "pollution" is used advisedly in this instance, since such heating of a waterway is not always necessarily detrimental. It is, however, true that the process is usually harmful, and thus the term has come into general use to describe the problem under consideration.

The magnitude of the Btu per hour so discharged into the waterways of the United States is astronomical. Although the temperature difference between the water received and that discharged seems small, it can strongly affect its biological system. And the general public often has a distorted view of the laws of thermodynamics and the causes of such heat rejection. This volume aims to provide a status report on the development of predictive analyses for temperature patterns in waterways with heated discharges, and to provide a concise reference work for those who wish to enter the field or need to use the results of such studies.

The papers range over a wide area of theory and practice, from theoretical mixing and system simulation to actual field measurements in real-time operations.

*304 pp., 6 x 9, illus. \$9.60 Mem. \$16.00 List*

TO ORDER WRITE: Publications Dept., AIAA, 1290 Avenue of the Americas, New York, N. Y. 10019